Interfaces structure and stress of gypsum (CaSO4·2H2O) penetration twins

Interfaces structure and stress of gypsum ($CaSO_4 \cdot 2H_2O$) penetration twins

Marco Rubbo*[1], Marco Bruno[1], Francesco Roberto Massaro[1] and Dino Aquilano[1]

ABSTRACT

In this work a structural analysis of the interface of penetration twins of gypsum is presented. The choice of the original composition plane of the twins is justified on energy and kinetic grounds. Beside, by static energy minimization, we calculate the relative bulk translations of the two crystals making the twin and the atomic movements at the interface of the bi-crystal. These structural details are described and the interface excess stress is evaluated.

1. Introduction

In a series of papers we assessed the structures and stability of Gypsum crystal faces and the energy of the twins of Gypsum [1-5]. In these works the singular flat (F) faces were identified as well as their low energy surface configuration. The studies were extended to the less stable stepped (S) and kinked (K) faces often observed in natural crystals and to the higher index faces belonging to the [001] zone. These works were preliminary to the study of gypsum twins allowing to identify the most likely composition planes and their surface configuration on energy grounds. Finally, we characterized the twin laws by their energy of formation so ranking the probability of occurrence of the contact and penetration twins; on the basis of several growth conditions, the morphology of each twin was predicted and compared with the observed one, when available. We gave the information required to manufacture the five penetration twins,[5] that is the orientation relations between the crystals adjoining on the 010 original composition plane (OCP). Our results seem in essential agreement with experimental findings [6,7] and can help to avoid some subtle pitfalls when identifying the twin laws.

Interfaces separating two crystals are studied since long time for basic knowledge and technological applications; the phases can be both bulky but also nano-phases as in case of epitaxy.[8] The structure of the interface is a record of the kinetic path of formation of the bi-crystal. Several mechanisms are invoked: a nucleation requiring a relatively high free energy barrier [9] or a displacive transition motivated by change of temperature, stress or some material property. Displacive transitions are modeled with the Landau-Ginsburg continuum model.[10-12] When the composition of the bi-crystal occurs on high index planes, a reconstruction of the interface by dislocations can decompose the boundary in planes of lower index: the inter-planar spacing large at the geometrical interface, decays, towards the bulk value, exponentially with the elastic strain field of the dislocations.[13] Starting from Hamiltonians describing atomic plane interactions, the oscillations of the inter-planar distances in the interfacial region can be calculated as a superposition of phonons with zero frequency.[13,14] A comprehensive presentation and review of elastic effects in surface physics can be found in the paper by Müller and Saul.[15]

Unlike previous works, we are concerned with growth twins where oscillations of the atomic plane distances, at the interface, result from static energy calculation based on the inter-atomic force field obtained by Adam.[16]

[1] Dipartimento di Scienze della Terra, Università degli Studi di Torino,
Via Valperga Caluso 35, I-10125 Torino, Italy.
*Corresponding author E-mail: marco.rubbo@unito.it; Fax: +390116705128; Tel: +390116705127

In this paper we extend the previous work with the analysis of the structural details determined by the relaxation process at the interface. We will rather concentrate on some other aspects of the twinning related to the PBC vectors anisotropy,[17] to the angular misfit and size of the mesh common to the two crystals and to the stress tensor at the interface between T (twinned) and P (parent) crystals. For the complexity of its structure, gypsum allows some insight on the role of short and long range forces on the probability of formation of twins on flat (F) and on stepped and kinked (S,K) faces.

2. Computer code and algorithms

To discuss the microscopic aspects of the interface relaxation we present the calculations made on the twin described by the $\bar{2}01$ law. As in our previous works,[3,4,18] calculations were performed with the "General Utility Lattice Program" GULP [19]; we considered geometry optimization achieved when gradient tolerance and the function tolerance, *gtol* and *ftol* a-dimensional parameters were smaller than 10^{-5} and 10^{-6}, respectively. To obtain high accuracy results the quest of a minimum of the static energy implemented the GULP options for the use of the Newton-Raphson method and Hessian calculation and inversion. Bi-crystal slabs sufficiently thick to avoid interactions among the surfaces of the twinned slab and the interface of the twin were generated by the program[20] GDISFurther details are given in the section "Computer code and algorithms" in the supporting information.

3. Generation and description of the twin

The P crystal is modeled as a slab consisting of 25 slices d_{020}. The 010 composition plane (OCP) on which the twin is composed can terminate exhibiting several stoichiometric and non polar configurations. We assumed a ~~regular~~ OCP surface terminated by one layer of structural water supposing that the twin fault involves the weakest bonds. The T crystal is generated from the P in two steps. First by a rotation of π about an axis of direction $[102]$, lying in the OCP. In this way the water bi-layer is re-constructed (see details of the interface in Fig. 1). Second, the T crystal is translated with respect to P. In this way, by inspection, we set a sensible initial interface configuration. The optimal configuration is then obtained by static energy minimization.[19] The P and T crystals have in common, on the 010 composition plane, a mesh of multiplicity 2 and have the common row $[102]$.With reference to Fig. 1, we describe the structure as a sequence of slices A, divided in layers A1, A2 and slices B (B1, B2), there are four layers of formula units in each A, B slice. The atoms in slice B are translated by $\frac{1}{2}[100]$ with respect to slice A. The layers of water molecules are within the slices A, B. The water molecules in layer B at the twin interface (B2 on the side of P and $B1_t$ twinned on the side of T crystal) experience the larger displacements.

In the direction of the diad axis, the SO_4 groups of one layer are piled on the Ca atoms of the adjacent layers. In the bulk the separation between the layers of equal type atoms is uneven. For instance Ca atoms in layer A1 and A2, as well as Ca in layers B1 and B2, are 5.123 Å apart, while Ca in layers A2-B1 and B2-A1 are 2.487 Å apart. Conversely, the oxygen of water molecules within layers A,B are in closer contact, 1.976 Å, than those in layers B2-A1, A2-B1 which are separated by 5.634 Å.

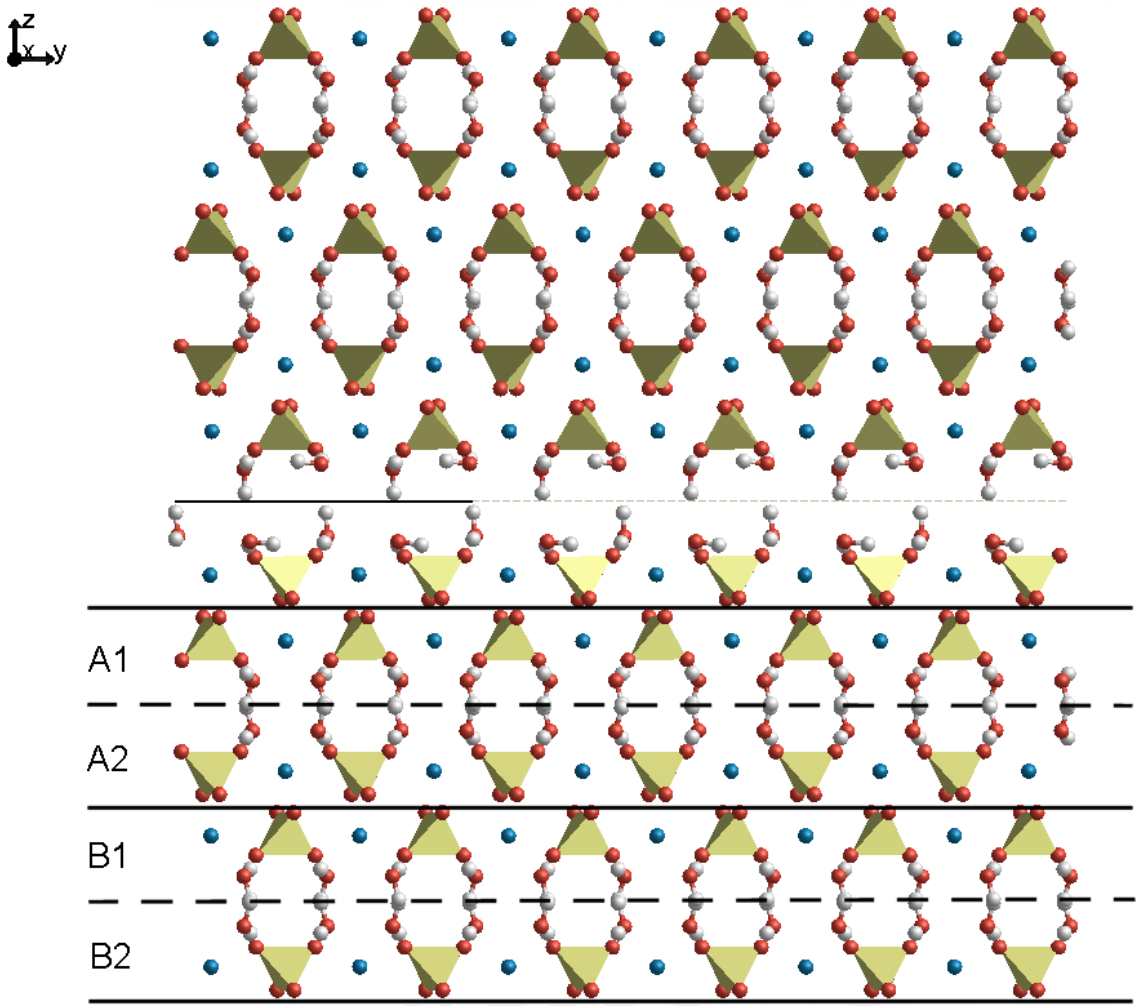

Figure 1. Structure of the twin. The projection is in direction [100] of the crystal P drawn in the lower part of the figure.

The positions of atoms in the bi-crystal are expressed in a common orthogonal base: the X axis is perpendicular to Y which, in turn, coincides with [102]; Z is parallel to [010]. The volume of the elementary translation cell so defined, is twice the volume of the crystallographic cell as the 2D coincidence mesh on 010 has double area. The transformation matrix from the reference chosen [22] is given in the supplementary information.

In order to describe the optimized interface expansion and the bulk translations of the T crystal relatively to the P one, variables Δ_α^l are defined as follows. Let be:

$$X_\alpha^{l,k} = {n_k}^{-1} \sum_{i=1}^{n_k} x_\alpha^{l,k} \ , \qquad \alpha = 1,3$$

where $x_\alpha^{l,k}$ are the atomic coordinates, the index k designates the atom species, l the layer number within the column representing the repeat 3D cell generating the twinned slab by translation, n_k the number of atom of specie k in every layer l.

In the following we will plot quantities $\Delta_\alpha^{lk} = X_\alpha^{l+1,k} - X_\alpha^{l,k}$ representing displacements of layers of atoms k. Considering structurally different the oxygen bonded to hydrogen from that bonded to sulfur we count five atomic species. The X_α^{lk} are then lumped together in a collective variable, C_α^l, expressing the mean coordinates associated to layer l:

$$C_\alpha^l = \frac{1}{5}\sum_{k=1}^{5} X_\alpha^{lk}$$

Finally $\Delta_\alpha^l = C_\alpha^{l+1} - C_\alpha^l$ represent the translation in the α direction of layer $l+1$ in respect to l. Due to the 2D periodic boundary conditions, no deformations occurs in 020 planes so, when $\alpha = 1,2$, Δ_α^l values represent mean relative layers translations; in direction [010] oscillations of inter-planar distances can occur, then $\frac{\Delta_3^l}{d_{020}}$ values represent the layer decomposition (see Figure 4; some example are reported in the paper by Müller and Saul [15]) of the intrinsic strain due to the interface relaxation (an analysis is given in the paper by Dingreville and Qu [21]), as it will be discussed in a following section.

4. Bulk translations and atomic movements at the interface

As reviewed by Sutton and Balluffi,[14] interface relaxation occurs by movements parallel and perpendicular to the interface which coincides with the OCP, in this case.

At the interface between P and T crystal the collective mean translations, occurring in directions $\Delta_1^l \; parallel\; to\; X$, $\Delta_2^l \; parallel\; to\; Y \equiv [102]$, decomposed by slices d_{020} thick are shown in Fig.2.

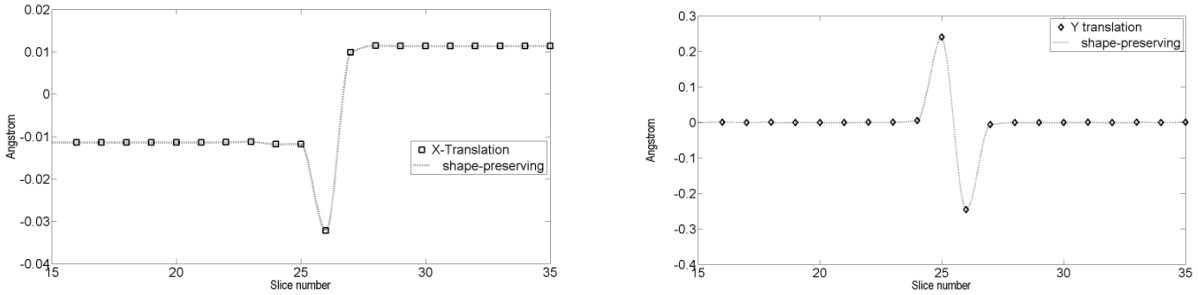

Fig.2 Relative translations of T and P crystals in the bulk and at the interface.

The mean bulk translations of T relatively to P crystal are very small in X direction, i.e. 0.02 Å, and are nil in Y direction. At the interface, perturbations involves about 6 slices, three on each crystal, but the amplitudes of the perturbations decay very rapidly; the perturbations are more ample in Y direction coinciding with the common row [102] : the two layers adjacent to a geometrical 010 plane separating the T from the P crystal are shifted ∓ 0.25 Å in respect to the bulk. These layers shifts optimize the atomic environments avoiding repulsions, but the consequences are the local breaking of symmetry as only the X,Y translations are conserved.

Mean slices expansions and compressions occur in direction [010]. As an example, in Figure 3 these are resolved layer by layer and by atomic species that are, from top to bottom, Ca, S and H. On the left column the separation of layers B1-A2, A1-B2 and $B1_t$ -$A2_t$, $A1_t$ -$B2_t$ in P and T crystal respectively are reported; on the right one the complementary separation between layers of kind A2-A1, B2-B1; the geometrical interface is between layers B2- $B1_t$. The absolute values of the compressions and expansions are significant at the interface where they amount to 0.5-1 Å.

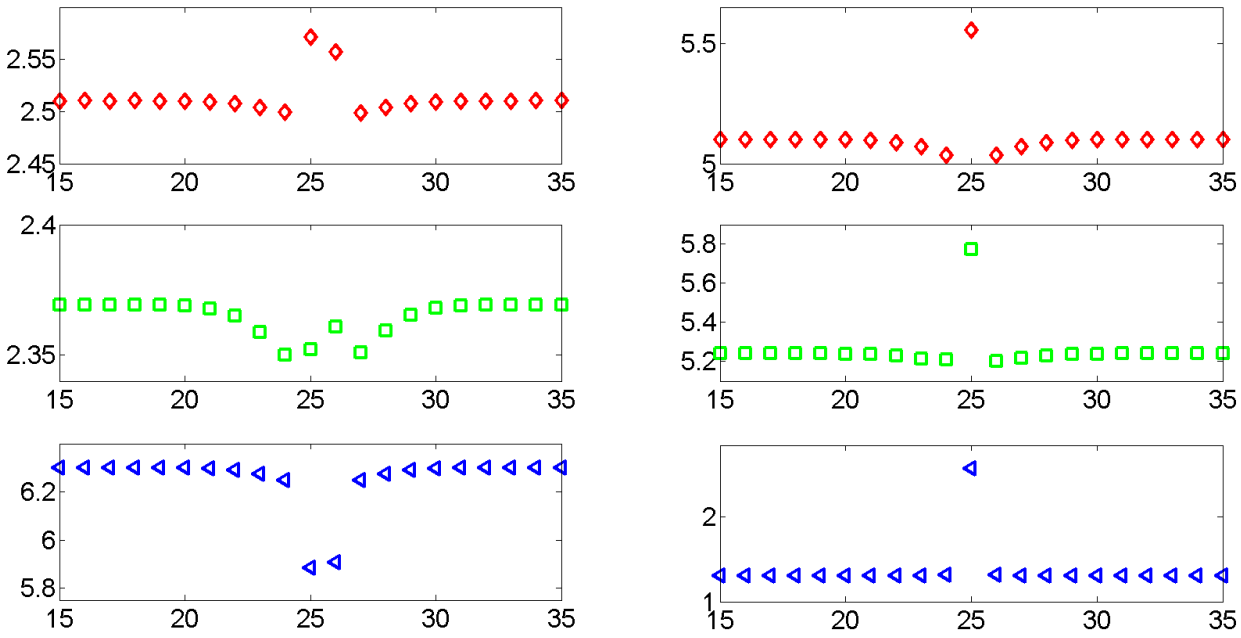

Fig.3 In the figure we show, as examples, the displacements of layers of Ca, S and H as a function of the slice number. See text for details.

Layers of different kind of atoms experience movements differing in direction and amplitude but, in the bulk, the mean separation of planes A-B of different atomic species is strictly the same and equal to d_{020}; this is shown in Figure 4 left panel, in case of sulfur layers. The perturbation of the mean equidistance d_{020} at the interface is shown in Figure 4 right panel. The pattern of Δ_3^l is similar to that of S planes but the oscillations are more ample.

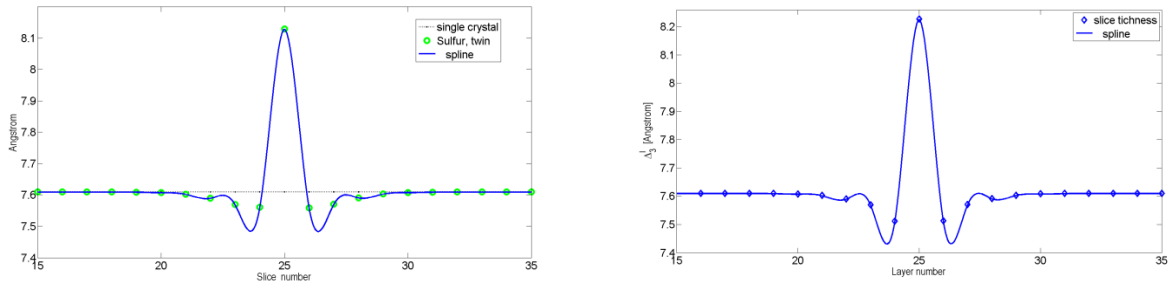

Fig.4 Left panel: separation of mean sulfur 010 planes. Right panel: Δ_3^l the mean separation of the slices 020.

Finally some distortions of the SO_4 tetrahedra and a rotation of the plane of two out of four water molecules occurs at the interface (Fig.1).

The deformations described could be biased by the force field used and different models, e.g. quantum-mechanical, would produce quantitatively different results. Numerical round off errors as well as flat energy hyper-surfaces can affect the significance of some results. However, as in any modeling and simulation works, a part of the interest consists also in pointing to potential singularities that could be not looked for or seen in a structural determination.

5. Surface stress

The interface deformations caused by the breaking of the symmetry of the forces through the interface, correspond to a new equilibrium characterized by an excess energy of the bi-crystal: a component of this excess can be ascribed to the elastic energy associated to the interface intrinsic strain. The bi-crystal excess energy (Extwin) per cell of thickness d_{020} (N_l is the number of d020 of the bi-crystal) is the difference between E_t the energy of a twinned slab per cell of volume V and that of an untwined one, E_n, [having the same number of atoms eliminerei questa specificazione] :

$$Ex_{twin} = \frac{E_t - E_n}{N_l} = 2.852e - 13\ erg$$

The mean elastic energy, in matrix notation, is :

$$E_{te} = \frac{1}{2} V \frac{\sum_i \sigma_i \in_i}{N_l}$$

where [V is the volume of a non deformed cell and eliminerei anche questo] $\sigma_i, \in_i$ are the stress and strain tensors calculated in every cell (layer). Spero sia chiaro che la colonna di N_l celle, di volume V ripetute periodicamente genera lo slab. Potrei considerare il volume V_i di ogni cella cui è associato lo stress ma la differenza suppongo sia trascurabile, mentre il confronto è sul volume ed energia dell'individuo "sano".

The summation is over the number of cells in the slab (bi-crystal). The strain is measured with reference to the non deformed crystal.

The mean elastic energy, E_{te} amounts to about 7 % of the excess energy of the twinned slab.

In order to estimate the stress tensor we use, as an approximation to the interface elastic constants, those measured and reported by Adam [16] for gypsum bulk. Taking as reference the configuration in the bulk of a not deformed crystal, and using the calculated strain in direction [010], we obtain the stresses resolved for each slice, shown in figure 5. The stresses σ_{11}, σ_{22} and σ_{33} are respectively in X, Y≡ [102], and Z ≡ [010] directions.

The stress parallel to 010 are mainly localized in the two slices on either side of the plane bisecting the bi-crystal, while the oscillation of the stress component σ_{33} occurs over the slices from 20 to 30. Apart from the central one (labeled 25) each slice experiences a compression.

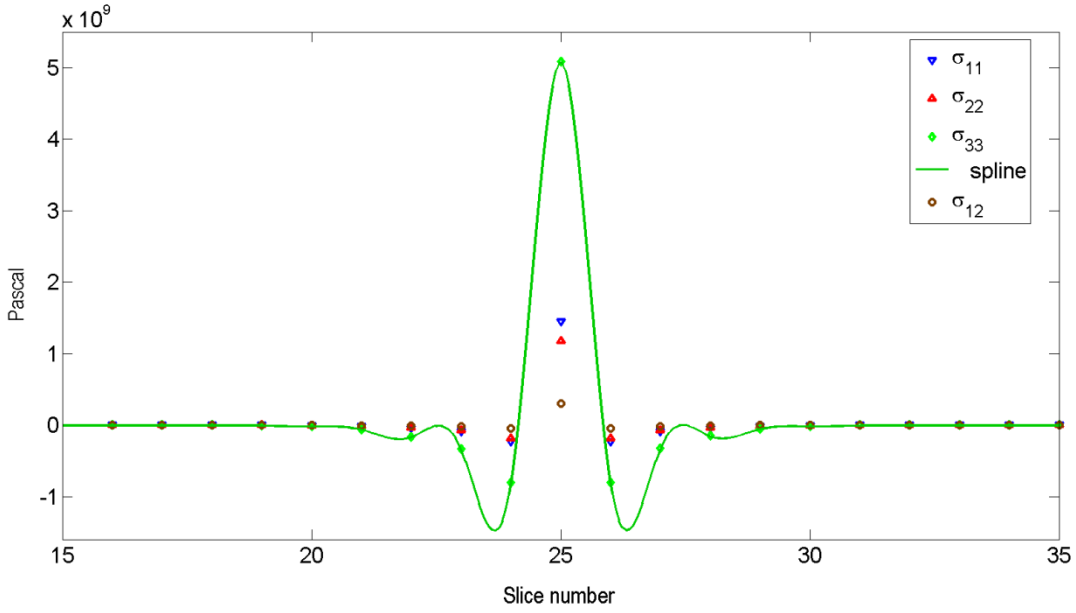

Fig.5 Slice decomposition of the stress at the 010 interface between T and P crystals.

The stress of the interface are estimated integrating the stress excess of the slices over the interface thickness (from slice 17 to 33) [15]:

$$s_{ij} = \frac{1}{A}\left[\sum_{k=n1}^{n2} \sigma_{ij}\,(k)\delta V(k) - \sigma_{ij}^{P} V^{P} - \sigma_{ij}^{T} V^{T}\right]$$

A and $\delta V(k)$ are the interface surface and the volume of each slice, respectively. Accounting for the numerical noise constrained by the values of *ftol* and *gtol* defined above, the strain in the bulk of T and P crystals are zero, so the stress in the bulk are $\sigma_{ij}^{P} = \sigma_{ij}^{T} = 0$ as well; it follows that the resulting excess stress is a traction in every direction with s_{22} smaller than s_{11}; a small shear stress arise in the plane 010.
In table 1 the relevant values for the twin $\bar{2}01$ are reported in $erg\ cm^{-2}$.

γ_{twin}	s_{11}	s_{22}	s_{33}	s_{12}
2171	518	422	1821	109

Table 1. Twin law $\bar{2}01$: interfacial energy and excess stress.

6. Conclusion

All penetration twins are composed on 010: it is also a cleavage plane and the corresponding face has character F. The geometrical plane through the interface between T and P crystals of all penetrations twins evenly partitions the layers of water between the two halves of the slab. No strong periodic bond chains transverse the face and the stiffness in the direction [010] is the lowest, as expected. The maximum mean expansion is of the order of 10^{-2} Å in case of the $10\bar{1}$ and 100 penetration twins as well as in case of the contact twin described by the law 100, but individual plane of atoms at the interface of the 100 penetration twins experience higher displacements. Conversely the expansion is of the order 10^{-1} Å in twin $20\bar{1}$. The $20\bar{1}$ twin energy is two order of magnitude greater than $10\bar{1}$. The 100 penetration twin energy is one order of magnitude greater than $10\bar{1}$.[5] Those among the penetration twin having the smaller energy of formation show the minor expansion of the lattice in direction [010]. These figures gives an idea about repulsive forces across the interface.

The $10\bar{1}$ penetration twin has the lowest obliquity of the 2D coincidence mesh and the highest mesh surface. The greater common mesh allows a greater orientation freedom of groups of atom and contribute to minimize short range repulsions and the total energy.

We have also to compare contact and penetration twins: it results that the energy of contact twins is in mean lower than that of penetration ones as the coincident site lattices mesh have no obliquity. Moreover, being the composition planes parallel to S or K faces, saturation of bonds trough the interface can easier occur. As S faces may occur at high supersaturation growth, only in such situations a twinned 2D nucleus can form.

From this study we may infer some properties of nanocrystals. A twinned 2D nucleus of gypsum cannot be considered a 2D Wulff crystal[23] as a size dependent stress sets in at the interface: as far as we know, this has only been considered in works on epitaxy, as described by Müller, Kern and co-workers.[15,24]
As reported in a previous work, [5] the optimal surface of the 2D mesh common to T and P crystals constrains the number of formula units necessary to build a stable nucleus. Therefore, in growth from solution, the kind of penetration twins that form depends on the crystallization conditions: e.g. twinned nuclei d_{020} thick, having a higher surface coincidence mesh can occur only at low supersaturation.

We also expect that the anisotropy of the affinity of crystallization[25] on the lateral faces of the twinned nuclei is strongly enhanced by elastic effects. However to evaluate quantitatively these effects, calculations on finite size nuclei should be performed.

References

1 F.R.Massaro, M.Rubbo, D. Aquilano, *Cryst.Growth Des.*, 2010**, 10**, 2870-2878.
2 F.R.Massaro, M.Rubbo, D. Aquilano, *Cryst.Growth Des.*, 2011**, 11**, 1607-1614.
3 M.Rubbo, M. Bruno, D. Aquilano, *Cryst.Growth Des.*, 2011**, 11**, 2351-2357
4 M.Rubbo, M. Bruno, F.R. Massaro, D. Aquilano, *Cryst.Growth Des.*, 2012**, 12**, 264-270.
5 M.Rubbo, M. Bruno, F.R. Massaro, D. Aquilano, *Cryst.Growth Des.*, 2012**, 12,**3018-3024.
6 B.Simon, *Contribution à l'étude de la Formation des Macles de Croissance*, Thèse docteur ès-Sciences Physiques: Marseille, France, 1968.
7 R.Kern, B.Rehn, *C.R. Acad. Sci. Paris*, 1960, **251**, 1300-1302.
8 P.Müller, R. Kern, *Surface Science*, 2003, **529**, 59-94.
9 R. Kern, *Bull. Soc. franc. Minér. Crist.*, 1961, **LXXXIV**,292-311.
10 B. Houchmandzadeh, J. Lajzerowicz, E. Salje, *J. Phys.: Condens. Matter*, 1992, **4**, 9779–9794.
11 B.Houchmandzadeh, J. Lajzerowicz, E. Salje, *Phase Transitions*, 1992, **38**, 77-87.
12 W.T.Lee, M.T. Dove, E.K.Salje, *J. Phys.: Condens. Matter*, 2000**, 12**, 9829–9841.
13 G.Allan, *Prog. Surf. Sci.*, 1987, **25**, 43–56.
14 A.P.Sutton, R.W. Balluffi *Interfaces in Crystalline Materials*, Clarendon Press: Oxford 2006.
15 P.Müller, A.Saul, *Surf.Science Reports*, 2004, **54**, 157-258.
16 C.D.Adam, J. *Solid State Chem.*, 2003, **174**, 141–151.
17 P.Hartman, In *Crystal Growth: An Introduction*,P. Hartman Ed., North Holland Publishing Co.: Amsterdam, 1973 pp 367-402.
18 M.Bruno, F.R. Massaro, M. Rubbo, M. Prencipe, D. Aquilano, *Cryst.Growth Des.*, 2010 **10**, 3102-3109.
19 J.D.Gale, *Faraday Trans.*, 1997, **93**, 629–637.
20 S.Fleming, A.Rohl, *Z. Kristallogr.*, 2005, **220**, 580–584.
21 R.Dingreville, J. Qu, *Acta Materialia*, 2007**, 55**, 141-147.
22 W.F.De Jong, J. Bouman, *Z. Kristallogr.*, 1938**, 100**, 275-276.
23 R.Defay, I. Prigogine, *Tension Superficielle et Adsorption*, Desoer : Liège 1951
24 P. Müller, R. Kern, in *Stress and Strain in Epitaxy: theoretical concepts, measurements and applications*, M.Handbucken and J.P.Deville Eds., Elsevier, Amsterdam, 2001.
25 A.I.Rusanov, *Surf.Science Reports*, 2005, **58**, 111-239.